# Stability of relativistic surfatron acceleration

Anton Artemyev,[1] Dmitri Vainchtein,[2,1] Anatoly Neishtadt,[3,1] and Lev Zelenyi[1]
[1]*Space Research Institute, Moscow, Russia*
[2]*Department of Mechanical Engineering, Temple University, Philadelphia, Pennsylvania, USA*
[3]*Department of Mathematical Sciences, Loughborough University, Loughborough, United Kingdom*
(Received 25 January 2014; published 18 April 2014)

In this paper we consider the surfatron acceleration of relativistic charged particles by a strong electrostatic wave propagating in a transverse direction relative to the background magnetic field. We investigate how high-frequency fluctuations of the background magnetic field affect the process of the resonant acceleration. We show that the presence of fluctuations leads to particle escape from the surfatron resonance and illustrate that fluctuations of different components of the magnetic field have quite a distinct effect on the energy gained by particles. In the case of the same power density, the strongest effect corresponds to fluctuations of the component directed along the background magnetic field, while the effect of the component along the wave front is substantially weaker. This is more important for particles with a large velocity component along the background magnetic field. We demonstrate that the dynamics of particles can statistically be described in terms of the adiabatic invariant diffusion. We derive the corresponding diffusion equation and compare solutions of that equation with results obtained by the explicit particle tracing.

DOI: 10.1103/PhysRevE.89.043106 PACS number(s): 52.35.−g, 52.20.Dq, 96.50.Fm

## I. INTRODUCTION

The resonant wave-particle interaction is one of the most challenging problems of plasma physics and has numerous applications. There are two main effects of such interaction: scattering of particles by waves and capture of particles by a wave [1]. Both effects have many manifestations (see [2–4]), but of all the mechanisms of acceleration of captured particles, the surfatron mechanism is probably the simplest and the most effective one. The term "surfatron" acceleration was introduced in [5], where the resonant interaction of relativistic electrons with an electrostatic wave in the presence of a weak background magnetic field was considered. Electrons captured by the wave move with the wave and are accelerated along the wave front. This type of motion gives rise to the name of this process, i.e., "surfatron."

Classical surfatron acceleration corresponds to the plasma configurations typical for two problems: the Landau damping in the presence of a weak magnetic field [6] and the resonant acceleration of particles by shock waves [7]. In both systems, charged particle acceleration along the wave front plays an important role. Starting from the first papers on the topic (e.g., [6]) and up to now [8,9], the influence of captured particles on Landau damping in the presence of a weak background magnetic field is actively studied. Particle acceleration along the wave front of a strong quasiperpendicular shock wave is considered to be a mechanism capable of describing the formation of high-energy populations [10]. Such a mechanism can occur in interplanetary shock waves (see [11–13] and references therein), in the solar corona [14,15], in planetary magnetospheres [16], and in various astrophysical shocks (see [17,18] and references therein). A similar mechanism of particle acceleration was found in laboratory experiments (so called "surface" acceleration; see [19]).

While the first investigations of the surfatron acceleration have been done for systems with electrostatic waves [5,6], the same effects of capture and acceleration can be found for electromagnetic waves propagating transversely to the background magnetic field [20–22]. Moreover, the effect of the surfatron acceleration of electrons by electromagnetic waves was reproduced in laboratory experiments [23]. For such systems, the mechanism of the particle acceleration is often called the "magnetic trapping" to distinguish it from the classical surfatron [24]. However, there is an important difference between the systems with electrostatic and electromagnetic waves. Electromagnetic waves can capture nonrelativistic particles into the regime of unlimited acceleration [22,25], while capture by electrostatic waves is unlimited only for relativistic particles [5,26–28].

There are several generalizations of the mechanism of the surfatron acceleration for more complex systems: effects of wave front curvature were considered in [29]; it was shown that the surfatron mechanism can be realized in systems with a curved background magnetic field [30]; the combination of the surfatron acceleration with gyroresonances was investigated in [31]; effects of the obliqueness of the wave propagation relative to the background magnetic field for electrostatic wave [21,27] and electromagnetic wave [32–34] were also investigated.

The surfatron acceleration is a consequence of capture into resonance, which is a fine resonant effect of the wave-particle interaction. Thus the peculiarities of captured particle motion could be expected to be very sensitive to any fluctuations of system parameters, such as the magnitude of the background magnetic field. Stability of the captured motion is the topic of this paper. It was shown before for the system where nonrelativistic particles were trapped by an electromagnetic wave that fast fluctuations of the background magnetic field put the upper limit on the duration of the captured motion and reduced the corresponding energy gain [35]. In the present paper we consider effects of magnetic field fluctuations on the classical electrostatic surfatron acceleration of relativistic particles.

## II. MAIN EQUATIONS

We consider the dynamics of relativistic particles in the system with the background magnetic field $B_0$ directed along

 

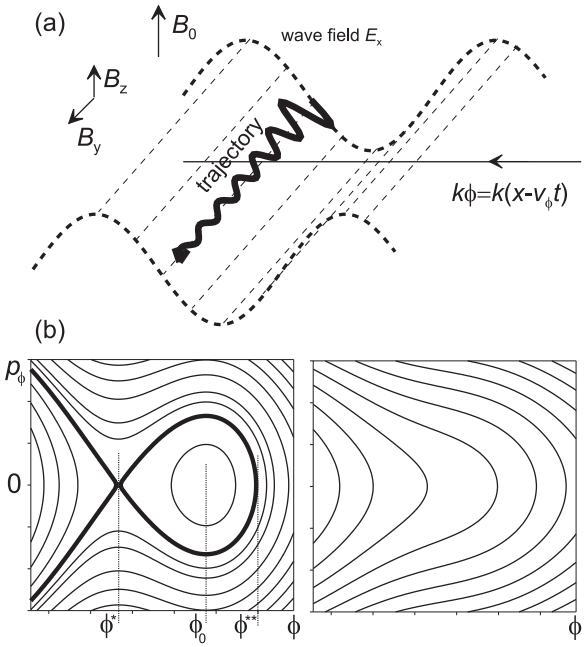


FIG. 1. (a) Schematic view of the system. (b) Phase portraits on the resonance plane.

the $z$ axis and the electrostatic wave defined by the potential $\varphi = \Phi_0 \sin(k\phi)$. Here phase $\phi = x - v_\phi t$; $k$ and $v_\phi$ are the wave number and the phase velocity, respectively. A schematic view of the system is presented in Fig. 1(a). We also take into account fluctuations of the magnetic field $\mathbf{B}_\Gamma = \{0, B_y, B_z\}$ (a corresponding vector potential is $\mathbf{A}_\Gamma = \{0, B_z x, -B_y x\}$). $B_x$ fluctuations are not taken into account (see the Discussion section for an explanation). Fluctuations are assumed to be weak compared with the background magnetic field. Without the loss of generality, the mean value of the fluctuations can be assumed to be zero: nonzero mean values of the $B_z$ distribution can be accounted for by changing $B_0$, while nonzero mean values of $B_y$ can be transformed into mean values of $B_z$ by a corresponding rotation of the coordinate system around the $x$ axis. For all numerical simulations we assumed the distributions of $B_z$, $B_x$ fluctuations to be Gaussian. However, the obtained analytical estimates are valid for non-Gaussian distributions as well. We assume that components of the magnetic field $\mathbf{B}_\Gamma$ change randomly with a period $\tau$, i.e., the value of $\mathbf{B}_\Gamma$ is constant during the time interval $\tau$, and at the moments $t_n = n\tau$ ($n = 0,1,2\ldots$) the value of $\mathbf{B}_\Gamma$ changes randomly. We consider systems where $\tau$ is the smallest of the time scales.

For the sake of the simplicity of the main equations we used a model of random magnetic field fluctuations that are synchronized over the whole space. Actually, that assumption is not important for our results and conclusions. In our numerical simulations, we independently defined the random magnetic field along each particle trajectory: in other words, we assumed that magnetic field, as a given particle sees it, changes randomly (regardless of what happens in the rest of the space). This simplification seems reasonable because we consider individual particle trajectories (to model dynamics of the particle ensemble we generate a new realization of a random magnetic field for each trajectory). In this case, magnetic field changes randomly with the frequency $1/\tau$ along a given trajectory. The proposed model implies that during every time interval $\sim\tau$ a particle covers the distance smaller than a spatial scale of inhomogeneity of the magnetic field fluctuations. This model can describe the charged particle interaction with high-frequency magnetic field fluctuations when the Doppler shift due to particle motion is smaller than fluctuation frequency. Such high-frequency fluctuations of magnetic field are observed in the near-Earth environment, [36], and, especially, at the vicinity of the Earth bow shock [37,38].

The Hamiltonian of a particle with charge $q$ and mass $m$ in the system under consideration can be written as

$$H = c\sqrt{c^2m^2 + p_x^2 + \Pi_z^2 + \Pi_y^2} + q\Phi_0 \sin(k\phi),$$
$$\Pi_z = p_z - \frac{q}{c} x B_y,$$
$$\Pi_y = p_y + \frac{q}{c} x(B_0 + B_z),$$

where $\mathbf{p} = \{p_x, p_y, p_z\}$ is the particle canonical momentum and $c$ is the speed of light. We use the following dimensionless variables: $\mathbf{p} \to \mathbf{p}/mc$, $u = v_\phi/c$, $\varphi_0 = q\Phi_0/mc^2$, $H \to H/mc^2$, $\mathbf{r} \to \mathbf{r}\Omega_0/c$, $k \to kc/\Omega_0$, $t \to \Omega_0 t$, $\mathbf{b} = \mathbf{B}_\Gamma/B_0$ where $\Omega_0 = qB_0/mc$ is the Larmor frequency. Because $\varphi_0$ is constant, changes (growth) in $\gamma$ correspond to the increase of the particle energy. For the numerical simulations presented in the paper we used $\tau\Omega_0 = 10^{-2}$. We consider dynamics of high-energy particles whose Larmor radius is much larger than the wavelength, which means $k \gg 1$, while the corresponding phase velocity of the wave is $u < 1$.

In dimensionless variables the Hamiltonian takes the form

$$H = \sqrt{1 + p_x^2 + (p_z - x b_y)^2 + [p_y + x(1 + b_z)]^2} + \varphi_0 \sin(k\phi). \quad (1)$$

Because Hamiltonian (1) does not depend on the $y$ and $z$ coordinates, we have $p_y = \text{const}$, $p_z = \text{const}$. The transformation $x \to x - p_y$ effectively replaces the term $p_y$ in the Hamiltonian with the terms of order $p_y b_y$ and $p_y b_z$. Both of these terms are small as $|\mathbf{b}| \ll 1$ and they do not depend on $x$ (we show below that $x$ grows significantly). Thus, we can neglect them. As a result, $p_y$ disappears from the Hamiltonian. However, unlike $p_y$, in a general case $p_z$ cannot be excluded from the Hamiltonian in the similar manner: the Hamiltonian does not depend on $p_z$ only for the system with $b_y = 0$.

After the terms with $p_y$ are removed from the Hamiltonian (1), the equations of motion become

$$\gamma \dot{x} = p_x,$$
$$\gamma \dot{p}_x = b_y(p_z - x b_y) - x(1 + b_z)^2 + \gamma k \varphi_0 \cos(k\phi),$$

where

$$\gamma = H - \varphi_0 \sin(k\phi) = \sqrt{1 + p_x^2 + (p_z - x b_y)^2 + x^2(1 + b_z)^2}.$$

### III. THE SYSTEM WITHOUT MAGNETIC FIELD FLUCTUATIONS

We start by considering the system without fluctuations of the magnetic field ($\mathbf{b} = 0$). In this case the Hamiltonian is

$$H = \sqrt{1 + p_x^2 + x^2} + \varphi_0 \sin(k\phi).$$

The corresponding equations of motion are

$$\begin{aligned} \gamma \dot{x} &= p_x, \\ \gamma \dot{p}_x &= -x - k\varphi_0 \gamma \cos(k\phi), \end{aligned} \tag{2}$$

where $\gamma = \sqrt{1 + p_x^2 + x^2}$ and $\phi = x - ut$. Thus we have the system with one and a half degrees of freedom. We use the generating function $M = (x - ut)P_\phi + xP_x$ to introduce new variables $(x, P_x)$, $(\phi, P_\phi)$:

$$\begin{aligned} p_x &= \frac{\partial M}{\partial x} = P_\phi + P_x, \quad \phi = \frac{\partial M}{\partial P_\phi} = (x - ut), \\ K &= \sqrt{1 + p_x^2 + x^2} + \varphi_0 \sin(k\phi) + \frac{\partial M}{\partial t} \\ &= \sqrt{1 + (P_\phi + P_x)^2 + x^2} + \varphi_0 \sin(k\phi) - uP_\phi, \end{aligned}$$

where $K$ is the new Hamiltonian. The corresponding equations of motion are

$$\begin{aligned} \gamma \dot{x} &= P_\phi + P_x, \\ \gamma \dot{P}_x &= -x, \\ \gamma \dot{\phi} &= P_\phi - \gamma u + P_x, \\ \dot{P}_\phi &= -k\varphi_0 \cos(k\phi) \end{aligned}$$

and

$$\gamma = \sqrt{1 + (P_\phi + P_x)^2 + x^2}.$$

In the vicinity of the Cherenkov resonance ($\dot{\phi} \approx 0$) we have $P_\phi + P_x = \gamma u$. Substituting this expression into the above expression for $\gamma$, we obtain $\gamma = \sqrt{1 + u^2\gamma^2 + x^2}$. This equation has the solution $\gamma = \gamma_\phi \sqrt{1 + x^2}$ where $\gamma_\phi = 1/\sqrt{1 - u^2}$. This is the expression for $\gamma$ in the resonance, while the system of equations acquires the form

$$\begin{aligned} \dot{x} &= u, \\ \gamma \dot{P}_x &= -x, \\ (\dot{\phi} + u)\sqrt{1 + x^2}/\sqrt{1 - (\dot{\phi} + u)^2} &= P_\phi + P_x, \\ \dot{P}_\phi &= -k\varphi_0 \cos(k\phi). \end{aligned} \tag{3}$$

The third equation can be expanded around $\dot{\phi} = 0$ as

$$\gamma u + \gamma_\phi^2 \gamma \dot{\phi} = P_\phi + P_x.$$

We introduce the new variable $p_\phi = P_\phi - P_\phi^{\text{res}}$, where $P_\phi^{\text{res}} = \gamma u - P_x$, and rewrite the last two equations in (3) as

$$\begin{aligned} \gamma \gamma_\phi^2 \dot{\phi} &= p_\phi, \\ \dot{p}_\phi &= -x\gamma_\phi^2/\gamma - k\varphi_0 \cos(k\phi). \end{aligned} \tag{4}$$

To derive these equations we kept terms $\sim\dot{\phi}$ and neglected the terms $\sim\dot{\phi}^2$ (see Appendix B and Ref. [25]). We also took into account that $k\phi$ changes substantially faster than $x$ and $\gamma$ due to the condition $k \gg 1$.

System (4) corresponds to Hamiltonian

$$H_\phi = \frac{1}{2\gamma\gamma_\phi^2} p_\phi^2 + \frac{x\gamma_\phi^2}{\gamma}\phi + \varphi_0 \sin(k\phi) \tag{5}$$

with $(\phi, p_\phi)$ being a canonical couple. The phase portrait of this system is shown in Fig. 1(b) for $x > 0$. One can see that for $x\gamma_\phi^2/\gamma < k\varphi_0$ (left panel) there are closed trajectories in the phase plane $(\phi, p_\phi)$, while for $x\gamma_\phi^2/\gamma > k\varphi_0$ (right panel) all trajectories are open. Particles moving along closed trajectories oscillate around the resonance $p_\phi = 0$. The separatrix (shown by the solid curve) separates closed and open trajectories in the phase plane. If the area $S$ surrounded by the separatrix grows with time, new particles can be captured into the resonance region. The expression for $S$ has the form

$$\begin{aligned} S = \oint p_\phi d\phi &= \gamma_\phi \sqrt{8\gamma} \\ &\times \int_{\phi^*}^{\phi^{**}} \sqrt{\frac{x}{\gamma}\gamma_\phi^2(\phi^* - \phi) + \varphi_0 \sin(k\phi^*) - \varphi_0 \sin(k\phi)} d\phi, \end{aligned} \tag{6}$$

where $(\phi^*, \phi^{**})$ are turning points of trapped particles moving along the separatrix; see Fig. 1(b).

For closed trajectories we can introduce the adiabatic invariant as

$$\begin{aligned} I_\phi = \oint p_\phi d\phi &= \gamma_\phi \sqrt{2\gamma} \\ &\times \oint \sqrt{H_\phi - \frac{x}{\gamma}\gamma_\phi^2 \phi - \varphi_0 \sin(k\phi)} d\phi, \end{aligned}$$

where the integration is performed along trajectories in the phase plane $(\phi, p_\phi)$ [see Fig. 1(b)]. Conservation of $I_\phi$ guarantees the perpetuity of capture of particles in the resonance region: due to the growth of $S$, after capture particle trajectories go away from the separatrix and cannot cross it again. If the condition $x\gamma_\phi^2/\gamma < k\varphi_0$ is satisfied for $x \to \infty$ (i.e., $\gamma_\phi < k\varphi_0$), then once captured the particles stay in the resonance forever [5].

An example of a particle trajectory obtained by numerical integration of system (2) is presented in Fig. 2. Initially the particle rotates around Larmor trajectory with approximately constant energy $\gamma \approx$ const (energy fluctuations correspond to variations of the electrostatic field $\sim\varphi_0 \cos\phi$). After a certain time, the particle is captured by the wave and starts moving with the wave ($\dot{x} \approx u$). The particle energy $\gamma$ grows linearly with time $\gamma \sim (ut)$. The invariant $I_\phi$ is conserved, while the area surrounded by the separatrix $S$ grows with time as $S \sim \sqrt{\gamma} \sim (ut)^{1/2}$; see [35]. This is the classical surfatron acceleration discovered in [5] and described by many authors (see, e.g., [21,26,27]).

In the course of acceleration, the particle trajectory in the phase plane $(\phi, p_\phi)$ evolves [see panel Fig. 2(d)]. The amplitude of oscillations in $\phi$ decreases (the particle goes down to the bottom of the potential well). Thus, together with the conservation of $I_\phi$, it yields the increase of the amplitude of $p_\phi$ oscillations.

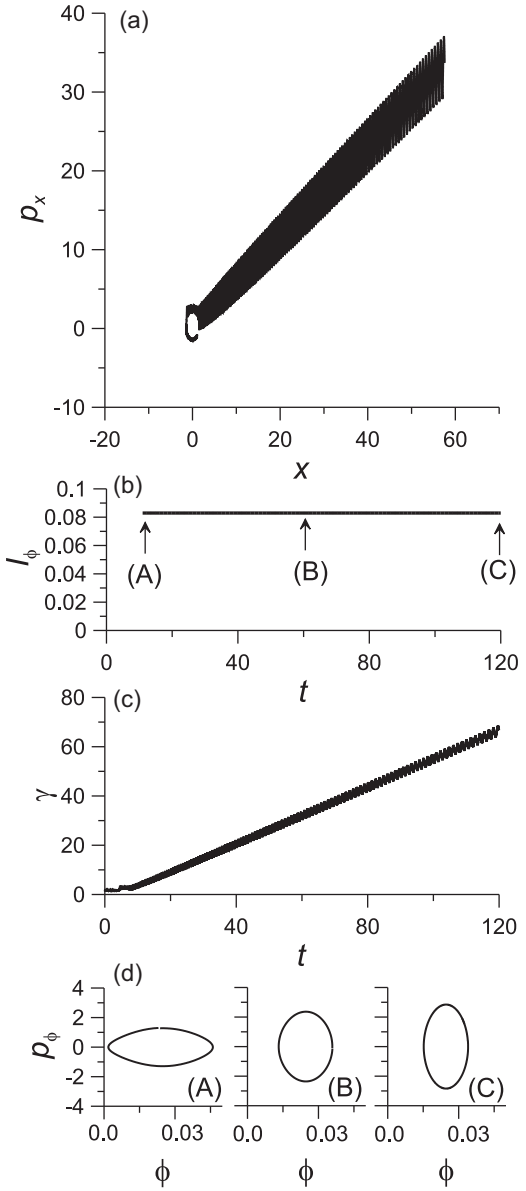


FIG. 2. A characteristic particle trajectory in the state of capture in the absence of fluctuations. (a) Projection on the $(x, p_x)$ plane. (b) The adiabatic invariant $I_\phi$ for time interval in capture. (c) The particle energy $\gamma$ as a function of time. (d) Three fragments of the particle trajectory in the $(\phi, p_\phi)$ plane.

Oscillations of captured particles in the $(p_\phi,\phi)$ plane result in oscillations of $(x,\dot{x})$ around the resonant values $(u_\phi t,u_\phi)$. To estimate a frequency of these oscillations, $\Omega_\phi$, we expand Hamiltonian $H_\phi$ around the bottom of the potential well, $\phi_0$ [see Fig. 1(b)]:

$$H_\phi \approx \frac{1}{2\gamma\gamma_\phi^2}p_\phi^2 - \frac{1}{2}k^2\varphi_0\sin(k\phi_0)(\phi-\phi_0)^2.$$

From this expression we obtain

$$\Omega_\phi \approx \sqrt{k^2\varphi_0/\gamma\gamma_\phi^2}, \tag{7}$$

i.e., the frequency of oscillations decays with time as $\sim 1/\sqrt{ut}$.

## IV. ROLE OF MAGNETIC FIELD FLUCTUATIONS

In this section we describe effects of magnetic field fluctuations on particle acceleration. We consider separately $b_z \neq 0$ and $b_y \neq 0$ fluctuations. These fluctuations can be described by the two-dimensional system with $(x, p_x)$ and $(\phi, P_\phi)$ variables.

The persistence of the particle acceleration is a consequence of the conservation of the adiabatic invariant $I_\phi$. To consider effects of fluctuations we describe evolution of $I_\phi$ in systems with finite $b_z$ or $b_y$. We show that every (random) change of $b_z$ or $b_y$ field causes a corresponding jump of the adiabatic invariant, $\Delta I_\phi$. In the following three subsections we show effects of magnetic field fluctuations on individual trajectories and derive the expressions for $\Delta I_\phi$. We consider the systems with $b_y \neq 0$ for particles with $p_z \sim 0$ and with finite $p_z$ separately.

Destruction of the adiabatic invariant $I_\phi$ may result in particle escape from the resonance with the wave. Thus, magnetic field fluctuations limit the time which particles spend in the resonance. This effect resembles the well known effect of resonance broadening when the particle diffusion due to the field fluctuations results in the limitation of time of wave-particle resonant interaction [39].

As magnetic field fluctuations are random, any individual trajectory cannot give a reliable estimate of the overall particle energization. To obtain typical energy of accelerated particles, we considered a particle ensemble. For each set of parameters, we numerically integrated $10^4$ trajectories—each corresponding to an individual particle. Initially all the particles were located in the resonance region with closed trajectories in the $(\phi, p_\phi)$ plane [see Fig. 1(b)]. As different particles gets captured at different time moments, each particle experiences a different sequence of fluctuations. Therefore, for each trajectory we generated a new realization of random values of the magnetic field fluctuations $b$. Each trajectory was integrated until the particle escaped from the resonance and its final (exit) energy was recorded. Then the final energy distribution was assembled.

### A. Influence of fluctuations of $B_z$ component

We start with the system with $b_z \neq 0$ and $b_y = 0$. In this case the Hamiltonian can be written as

$$H = \gamma + \varphi_0\sin(k\phi),$$
$$\gamma = \sqrt{1 + p_x^2 + x^2(1+b_z)^2}.$$

The corresponding equations of motion are

$$\begin{aligned}\gamma\dot{x} &= p_x,\\ \gamma\dot{p}_x &= -x(1+b_z)^2 - k\varphi_0\gamma\cos(k\phi).\end{aligned} \tag{8}$$

We use the same generating function $M = (x-ut)P_\phi + xP_x$ to introduce new variables $P_x$ and $P_\phi$ and Hamiltonian $K$ as in the previous section. Equations of motion become

$$\begin{aligned}\gamma\dot{x} &= P_\phi + P_x,\\ \gamma\dot{P}_x &= -x(1+b_z)^2,\\ \gamma\dot{\phi} &= P_\phi - \gamma u + P_x,\\ \dot{P}_\phi &= -k\varphi_0\cos(k\phi),\end{aligned}$$

where

$$\gamma = \sqrt{1 + (P_\phi + P_x)^2 + x^2(1 + b_z)^2}.$$

In the vicinity of the resonance $\dot{\phi} = 0$ we have

$$\begin{aligned} \dot{x} &= u, \\ \gamma P_x &= -x(1 + b_z)^2, \\ \gamma\dot{\phi} &= P_\phi - \gamma u + P_x, \\ \dot{P}_\phi &= -k\varphi_0 \cos(k\phi), \end{aligned} \tag{9}$$

where we used $P_\phi + P_x \approx \gamma u$ to obtain $\gamma = \gamma_\phi\sqrt{1 + x^2(1 + b_z)^2}$ (see the previous section for details). In terms of $p_\phi = P_\phi - P_\phi^{\rm res}$ we can rewrite (9) as

$$\begin{aligned} \gamma\gamma_\phi^2\dot{\phi} &= p_\phi, \\ \dot{p}_\phi &= -x(1 + b_z)^2\gamma_\phi^2/\gamma - k\varphi_0 \cos(k\phi). \end{aligned}$$

This is a Hamiltonian system with Hamiltonian

$$H_\phi = \frac{1}{2\gamma\gamma_\phi^2}p_\phi^2 + \frac{x(1 + b_z)^2\gamma_\phi^2}{\gamma}\phi + \varphi_0 \sin(k\phi). \tag{10}$$

We assume that $I_\phi$ can be calculated for unperturbed system (5), while jumps of $I_\phi$ correspond to perturbation $\sim b_z$. To estimate the jump of the adiabatic invariant $\Delta I_\phi$ at a single change of the magnetic field, we use the expression $\Omega_\phi = 2\pi\,\partial H_\phi/\partial I_\phi$ [40], which yields $\Delta I_\phi \approx 2\pi\,\Delta H_\phi/\Omega_\phi$. Change of energy $\Delta H_\phi$ corresponds to terms $\sim b_z$ and can be estimated as the difference between Hamiltonians (5) and (10):

$$\Delta H_\phi = \frac{x\left(2b_z + b_z^2\right)\gamma_\phi^2}{\gamma}\Delta\phi.$$

As $\gamma\gamma_\phi^2\dot{\phi} = p_\phi$, see (5), we have $\Delta\phi = \tau p_\phi/(\gamma\gamma_\phi^2)$. As a result, we can derive the expression for $\Delta I_\phi$:

$$\begin{aligned} \Delta I_\phi &= \frac{2\pi}{\Omega_\phi}\frac{p_\phi}{\gamma^2}\left(2b_z + b_z^2\right)x\tau \\ &= \frac{2\pi}{\sqrt{\gamma_\phi^3 k^2\varphi_0}}\tau p_\phi\frac{\left(2b_z + b_z^2\right)x}{[1 + x^2(1 + b_z)^2]^{3/4}}. \end{aligned}$$

Here we can use an approximate expression (7) for the frequency of oscillations $\Omega_\phi$.

Assuming the statistical independence of $p_\phi$ and $b_z$, we obtain that the average jump is $\langle\Delta I_\phi\rangle \propto \oint p_\phi dt = 0$ and the variance of $\Delta I_\phi$ is

$$\mathrm{Var}(\Delta I_\phi) = \frac{(2\pi)^2}{\gamma_\phi^3 k^2\varphi_0}\tau^2\Gamma_z(x)\mathrm{Var}(p_\phi),$$

where

$$\Gamma_z(x) = \mathrm{Var}\left(\frac{\left(2b_z + b_z^2\right)x}{[1 + x^2(1 + b_z)^2]^{3/4}}\right).$$

Here we took into account that when the value of $k$ is large enough $x$ changes slowly (i.e., $x \approx$ const for one period of particle oscillation inside the resonance). Profiles of $\Gamma_z(x)$ for various $\sigma_z = \mathrm{Var}(b_z)$ are shown in Fig. 3 (we considered a Gaussian distribution of $b_z$). One can see that $\Gamma_z$ grows with

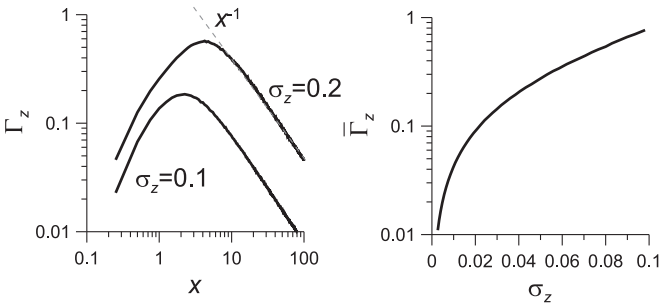


FIG. 3. (a) Profiles of the function $\Gamma_z(x)$. (b) The values of $\bar{\Gamma}_z$ as a function of $\sigma_z = \mathrm{Var}(b_z)$.

$x$ for small $x$. For small amplitudes of $b_z$ fluctuations the maximum of $\Gamma_z(x)$ is proportional to $\sim\sigma_z$.

For large $x$ the function $\Gamma_z(x)$ decreases as $1/x$:

$$\Gamma_z(x) \approx \frac{1}{x}\mathrm{Var}\left(\frac{2b_z + b_z^2}{(1 + b_z)^{3/2}}\right) = \frac{1}{x}\bar{\Gamma}_z.$$

We plot $\bar{\Gamma}_z$ as a function of $\sigma_z = \mathrm{Var}(b_z)$ in Fig. 3(b). Factor $1 + b_z$ in the denominator of $\bar{\Gamma}_z$ leads to a rapid increase of $\bar{\Gamma}_z$ with $\sigma_z$. This is drastically different from the nonrelativistic system, where $\bar{\Gamma}_z \sim \sigma_z$ (see [35]).

We use the definition of $I_\phi$ for unperturbed system to derive the expression for $\mathrm{Var}(p_\phi)$:

$$\frac{2\pi}{\Omega_\phi}\frac{1}{\gamma\gamma_\phi^2}\mathrm{Var}(p_\phi) \approx \oint\frac{p_\phi^2}{\gamma\gamma_\phi^2}dt = I_\phi.$$

Thus

$$\mathrm{Var}(\Delta I_\phi) = \frac{2\pi\gamma\tau^2}{\gamma_\phi k^2\varphi_0}\Omega_\phi I_\phi\Gamma_z(x) = \frac{2\pi\tau^2 I_\phi}{\gamma_\phi^2\sqrt{k^2\varphi_0}}\gamma^{1/2}\Gamma_z(x).$$

$\mathrm{Var}(\Delta I_\phi)$ depends on $x$ as

$$\mathrm{Var}(\Delta I_\phi) \sim \gamma\Omega_\phi\Gamma_z(x) \sim \gamma^{1/2}\Gamma_z(x).$$

The function $\gamma^{1/2}\Gamma_z(x)$ has the asymptote $\sim x^{-1/2}$. We finally get for large $x$

$$\mathrm{Var}(\Delta I_\phi) \approx \frac{2\pi}{\sqrt{\gamma_\phi k^2\varphi_0}}\tau^2\frac{I_\phi\bar{\Gamma}_z}{x^{1/2}}.$$

We arrived at a classical random walk of particles in the space $I_\phi > 0$. Recall that all the captured particles have the value of $I_\phi$ less than the value $S$ of the area under the separatrix. When $I_\phi$ for a certain particle trajectory reaches $S$, the corresponding particle leaves the resonance. To illustrate this effect we integrated system (8) numerically (see Fig. 4). Fig. 4(a) shows a characteristic particle trajectory in the $(x, p_x)$ plane: initially the particle rotates around the background magnetic field, then the particle is captured and starts moving along the resonant trajectory $x \approx ut$ and $p_x \approx u\gamma_\phi(ut)$. After a certain time the particle escapes from the resonance and starts rotating around the background magnetic field with an increased energy (the radius of the corresponding Larmor circle is larger than the initial radius). The evolution of the particle energy is shown in Fig. 4(c). Panel (b) demonstrates the evolution of the invariant $I_\phi$ (value of $S$ is shown by the grey curve). The adiabatic invariant $I_\phi$ randomly changes along the

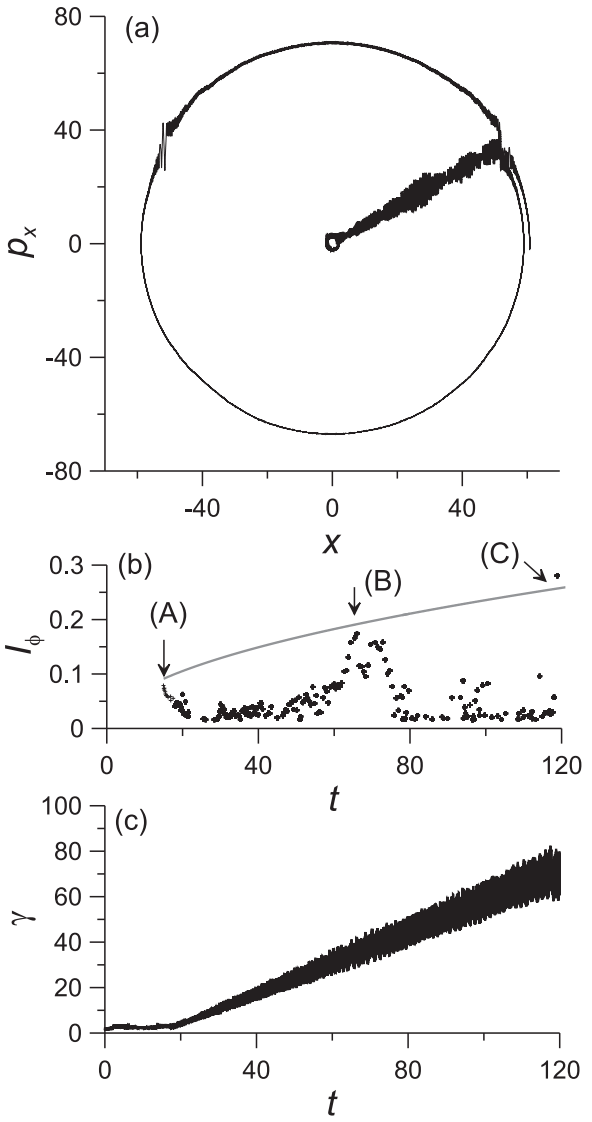


FIG. 4. A characteristic particle trajectory in the state of capture in the presence of fluctuations. (a) Projection on the $(x, p_x)$ plane. (b) The adiabatic invariant $I_\phi$ for the time interval in capture. The solid line is value of the area under separatrix $S$. (c) The particle energy $\gamma$ as a function of time. The parameters are $\sigma_z = 0.03$, $u = 0.5$, $k\varphi_0 = 20$, $k = 100$.

trajectory due to magnetic field fluctuations. One can see that the particle escapes from the resonance just when $I_\phi$ becomes larger than $S$. We show fragments of the particle trajectory in the $(\phi, p_\phi)$ phase plane in Fig. 5 for three moments of time marked in Fig. 4(b) by letters. Indeed, the area surrounded by trajectories (or the invariant $I_\phi$) grows with time [compare Fig. 5 and Fig. 2(d) where similar trajectories are shown for the system without magnetic field fluctuations].

The final energy distribution for $10^4$ trajectories—each corresponding to an individual particle—is presented in Fig. 6. One can see that the increase of the fluctuation level, $\sigma_z$, results in the decrease of the characteristic final energy gained by particles (i.e., the decrease of time which particles spend in capture).

### B. Influence of fluctuations of $B_y$ component: Particles with $p_z \sim 0$

In this section we consider the influence of $b_y$ fluctuations on acceleration of particles with $p_z \sim 0$. The corresponding Hamiltonian is

$$H = \gamma + \varphi_0 \sin(k\phi), \qquad \gamma = \sqrt{1 + p_x^2 + x^2\left(1 + b_y^2\right)}. \tag{11}$$

The change of variables with the same generating function as the one used in Sec. IV A leads to equations of motion

$$\gamma \dot{x} = P_\phi + P_x, \quad \gamma \dot{P}_x = -x\left(1 + b_y^2\right), \quad \gamma \dot{\phi} = P_\phi - \gamma u + P_x, \quad \dot{P}_\phi = -k\varphi_0 \cos(k\phi),$$

where

$$\gamma = \sqrt{1 + (P_\phi + P_x)^2 + x^2\left(1 + b_y^2\right)}.$$

In the vicinity of the resonance $\dot{\phi} = 0$ we have

$$\gamma\gamma_\phi^2\dot{\phi} = p_\phi, \qquad \dot{p}_\phi = -x\left(1 + b_y^2\right)\gamma_\phi^2/\gamma - k\varphi_0 \cos(k\phi),$$

where $p_\phi = P_\phi - P_\phi^{\rm res}$ and $P_\phi^{\rm res} = \gamma u - P_x$. This is a Hamiltonian system with the Hamiltonian

$$H_\phi = \frac{1}{2\gamma\gamma_\phi^2}p_\phi^2 + \frac{x\left(1 + b_y^2\right)\gamma_\phi^2}{\gamma}\phi + \varphi_0 \sin(k\phi).$$

Following Sec. IV A, we obtain the expression for the jump of the adiabatic invariant $\Delta I_\phi$:

$$\Delta I_\phi = \frac{2\pi}{\Omega_\phi}\frac{p_\phi}{\gamma^2}b_y^2 x\tau = \frac{2\pi}{\sqrt{\gamma_\phi^3 k^2\varphi_0}}\tau p_\phi \frac{b_y^2 x}{\left[1 + x^2\left(1 + b_y^2\right)\right]^{3/4}}.$$

Statistical independence of $p_\phi$ and $b_y$ values results in a zero value of averaged jump $\langle \Delta I_\phi \rangle \sim \int p_\phi dt = 0$. For the variance $\mathrm{Var}(\Delta I_\phi)$ we have

$$\mathrm{Var}(\Delta I_\phi) = \frac{(2\pi)^2}{\gamma_\phi^3 k^2\varphi_0}\tau^2 \mathrm{Var}(p_\phi)\Gamma_y(x) = \frac{2\pi}{\gamma_\phi k^2\varphi_0}\tau^2\gamma\Omega_\phi I_\phi \Gamma_y(x) = \frac{2\pi\tau^2 I_\phi}{\gamma_\phi^2\sqrt{k^2\varphi_0}}\gamma^{1/2}\Gamma_y(x),$$

where

$$\Gamma_y(x) = x^2 \mathrm{Var}\left(\frac{b_y^2}{\left[1 + x^2\left(1 + b_y^2\right)\right]^{3/4}}\right).$$

Here once again we assumed that $x$ changes slowly and $x \approx$ const during one period of particle oscillations in the resonance $\sim 2\pi/\Omega_\phi$.

Profiles of $\Gamma_y(x)$ are presented in Fig. 7(a) for various values of $\sigma_y = \mathrm{Var}(b_y)$. Comparison of Figs. 3 and 7(a) shows

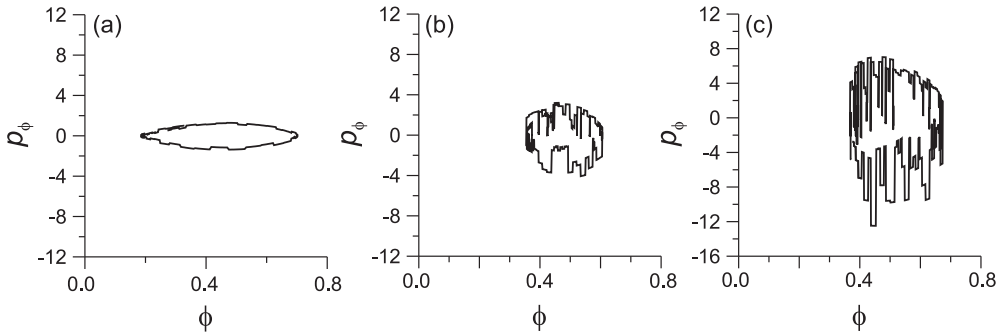


FIG. 5. Three fragments of the particle trajectory in the $(\phi, p_\phi)$ plane for the $A$, $B$, and $C$ moments of time indicated in Fig. 4.

that both functions $\Gamma_z(x)$ and $\Gamma_y(x)$ have similar profiles, but absolute values of $\Gamma_z(x)$ are substantially larger than values of $\Gamma_y(x)$. For example, for a small amplitude of $b_y$ fluctuations the maximum value of $\Gamma_y(x)$ is proportional to $\mathrm{Var}(b_y^2) \sim \sigma_y^2$. For large enough values of $x$, we have

$$\Gamma_y(x) \approx \frac{1}{x}\mathrm{Var}\left(\frac{b_y^2}{\left(1+b_y^2\right)^{3/4}}\right) = \frac{1}{x}\bar{\Gamma}_y$$

and

$$\mathrm{Var}(\Delta I_\phi) \approx \frac{2\pi}{\sqrt{\gamma_\phi k^2 \varphi_0}}\tau^2 \frac{I_\phi \bar{\Gamma}_y}{x^{1/2}}.$$

Characteristic profiles of $\bar{\Gamma}_y$ as a function of $\sigma_y$ is shown in Fig. 7(b).

Typical particle trajectories in the systems with $b_z$ and $b_y$ demonstrates the qualitatively similar behavior: we observe particle capture and escape from the resonance with a certain energy gain. The smallness of $\bar{\Gamma}_y$ in comparison with $\bar{\Gamma}_z$ should manifest itself in the energy distributions of a particle ensemble. We performed an integration of $10^4$ trajectories as was done in Sec. IV A. Final energy distributions are shown in Fig. 8. Comparison of Figs. 6 and 8 shows that for the same values $\sigma_z = \sigma_y = 0.08$ and $\sigma_z = \sigma_y = 0.12$ the maximum energies differ by more than one order of magnitude: particles are accelerated more effectively in the system with $b_z = 0$, $b_y \neq 0$ in comparison with the system with $b_z \neq 0$, $b_y = 0$.

### C. Influence of fluctuations of $B_y$ component: Particles with $p_z \neq 0$

In this section we consider the influence of $b_y$ fluctuations on acceleration of particles with finite values of $p_z$. The corresponding Hamiltonian is

$$H = \gamma + \varphi_0 \sin(k\phi),$$
$$\gamma = \sqrt{1 + p_x^2 + x^2 + (p_z - x b_y)^2} \tag{12}$$

and $p_z = \mathrm{const}$. Using a renormalization of Hamiltonian $H \to H/\sqrt{1+p_z^2}$, $(p_x, x) \to (p_x, x)/\sqrt{1+p_z^2}$, and $\varphi_0 \to \varphi_0/\sqrt{1+p_z^2}$, we get

$$H = \gamma + \varphi_0 \sin(kx - k v_\phi t),$$
$$\gamma = \sqrt{1 + p_x^2 + \left(1+b_y^2\right)(x - x_0)^2},$$
$$x_0 = b_y p_z / \left(1 + b_y^2\right).$$

Here we assumed that $b_y$ is small enough to use the approximation $1 + p_z^2/(1+b_y^2) \approx 1 + p_z^2$. The same transformations as in Sec. IV B result in equations of motion in the vicinity of

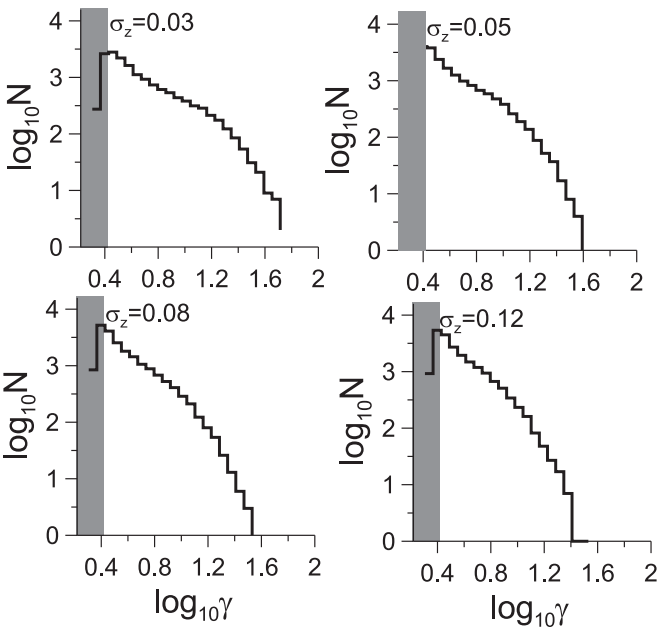


FIG. 6. Energy distributions for four values of $\sigma_z = \mathrm{Var}(b_z)$. The grey strips indicate the initial energy range.

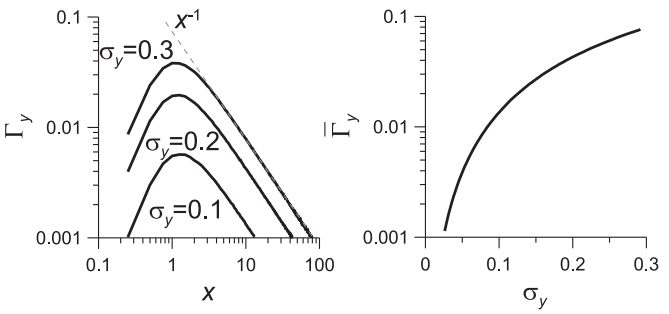


FIG. 7. (a) Profiles of the function $\Gamma_y(x)$. (b) The values of $\bar{\Gamma}_y$ as a function of $\sigma_y = \mathrm{Var}(b_y)$.

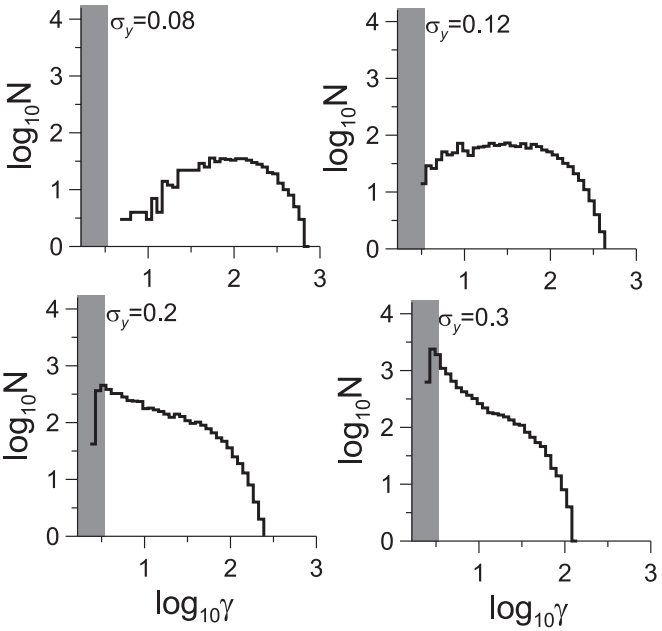


FIG. 8. Energy distributions for four values of $\sigma_y = \mathrm{Var}(b_y)$. The grey strips indicate the initial energy range.

the resonance $\dot{\phi} = 0$; we have

$$\gamma\gamma_\phi^2\dot{\phi} = p_\phi,$$
$$\dot{p}_\phi = -(x - x_0)\left(1 + b_y^2\right)\gamma_\phi^2/\gamma - k\varphi_0\cos(k\phi).$$

The corresponding Hamiltonian is

$$H_\phi = \frac{1}{2\gamma\gamma_\phi^2}p_\phi^2 + \frac{(x - x_0)\left(1 + b_y^2\right)\gamma_\phi^2}{\gamma}\phi + \varphi_0\sin(k\phi).$$

The jump of the adiabatic invariant $\Delta I_\phi$ is

$$\Delta I_\phi = \frac{2\pi}{\Omega_\phi}\frac{p_\phi}{\gamma^2}\left[b_y^2 x - x_0\left(1 + b_y^2\right)\right]\tau$$
$$\approx \frac{2\pi}{\sqrt{\gamma_\phi^3 k^2\varphi_0}}\tau p_\phi\frac{b_y^2 x - x_0}{\left[1 + x^2\left(1 + b_y^2\right)\right]^{3/4}}.$$

Here we took into account that $|b_y| \ll 1$ to exclude the constant term $b_y^2 x_0 \sim b_y^3$. For the variance $\mathrm{Var}(\Delta I_\phi)$ we have

$$\mathrm{Var}(\Delta I_\phi) = \frac{2\pi\tau^2\gamma\Omega_\phi I_\phi}{\gamma_\phi k^2\varphi_0}\Gamma_y(x, p_z) = \frac{2\pi\tau^2 I_\phi\sqrt{\gamma}}{\gamma_\phi^2\sqrt{k^2\varphi_0}}\Gamma_y(x, p_z),$$

where

$$\Gamma_y(x, p_z) = \mathrm{Var}\left(\frac{b_y^2 x - x_0}{\left[1 + x^2\left(1 + b_y^2\right)\right]^{3/4}}\right).$$

Profiles of $\Gamma_y(x, p_z)$ are shown in Fig. 9 for various values of $\sigma_y = \mathrm{Var}(b_y)$ and $p_z$. An increase of $p_z$ leads to larger values of $\Gamma_y(x, p_z)$ for small $x$ compared with $\Gamma_y(x, 0)$. For small $x$, large values of $\Gamma_y(x, p_z)$ result in particle escape from the resonance in the initial stage of acceleration. The function $\Gamma_y(x, p_z)$ has the same asymptote for large $x$ as $\Gamma_y(x, 0) \sim 1/x$. Therefore, the long-time evolution of the system does not depend on $p_z$. Similar to Sec. IV B, we performed the numerical

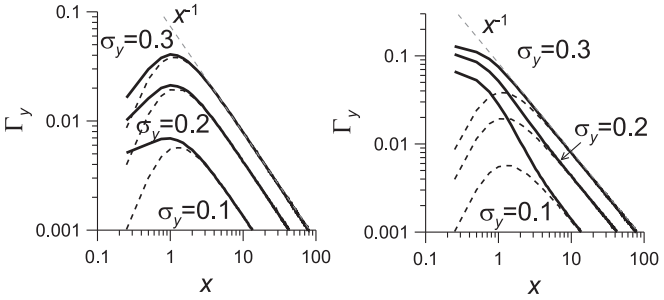


FIG. 9. Profiles of function $\Gamma_y(x, p_z)$ for $p_z = 0.25$ (left panel) and $p_z = 1$ (right panel). Black dotted curves correspond to the function $\Gamma_y(x)$ for $p_z = 0$.

integration of $10^4$ trajectories to assemble energy distributions (see Fig. 10). The comparison of the energy distributions for $p_z = 0.25$ and $p_z = 1.0$ confirms our conclusions: for $p_z = 1.0$ there is a large amount of particles which escaped from the resonance with small energies (i.e., in the beginning of acceleration). The distribution of particles which stay in resonance for a long time is similar for both values of $p_z$. (When normalized by the number of particles that were not released from the resonance immediately, the distribution for $p_z = 0$ and $p_z = 1.0$ almost overlap.) Moreover, the increase of $\sigma_y$ leads to the decrease of the duration of particle acceleration. As a result, for large $\sigma_y$ there is no difference between the energy distributions obtained for $p_z = 0.25$ and $p_z = 1.0$.

## V. DIFFUSION EQUATION

Due to a random nature of magnetic field fluctuations, a behavior of $I_\phi$ for any individual trajectory cannot give

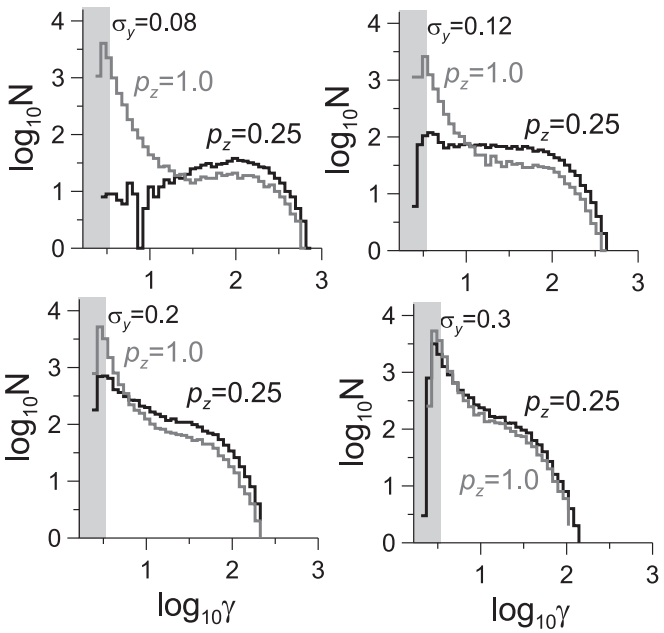


FIG. 10. Energy distributions for four values of $\sigma_y = \mathrm{Var}(b_y)$ and two values of $p_z$. The grey strips indicate the initial energy range.

any statistically significant quantitative information. Thus, we need to consider an ensemble of trajectories with a certain distribution of adiabatic invariants $F(I_\phi)$. The evolution of $F(I_\phi)$ can be described by the diffusion equation

$$\frac{\partial F}{\partial t} = \frac{\partial}{\partial I_\phi}\left(D_{I_\phi I_\phi}\frac{\partial F}{\partial I_\phi}\right)$$

with the diffusion coefficient $D_{I_\phi I_\phi} = \mathrm{Var}(\Delta I_\phi)/\tau$.

For the nonrelativistic system it was shown that the distribution of the gained energy obtained from integration of full trajectories for the particle ensemble is very similar to one obtained from consideration of the ensemble of trajectories in the one-dimensional space of invariants $I_\phi$ with random jumps $\Delta I_\phi$, [35]. In this section, we consider the diffusion equation for the relativistic system with $b_z \neq 0$ and $b_y \neq 0$ fluctuations. For the sake of simplicity we consider here only systems with $p_z \sim 0$. The diffusion coefficient is given by

$$D_{I_\phi I_\phi} \approx \frac{2\pi\tau I_\phi}{\gamma_\phi^2\sqrt{k^2\varphi_0}}\gamma^{1/2}(t)\Gamma(t)$$

and $\Gamma(t) = \Gamma_{z,y}(t)$. In the course of acceleration the particle energy $\gamma$ grows almost linearly with time ($\gamma \approx \gamma_\phi u t$). Thus it is convenient to introduce the time scale $t_0 = \gamma_0/\gamma_\phi u$ where $\gamma_0$ is the initial energy. In this case the area surrounded by the separatrix can be written as $S \sim \sqrt{\gamma} = S_0\sqrt{t/t_0}$ where $S_0$ is the value of $S$ at the initial moment of time. At this moment the adiabatic invariants of all the particles are equal to $S_0$ and we can introduce the initial distribution as $F_{t=t_0} = \delta(I_\phi/S_0 - 1)$ with $\delta(\cdot)$ is the Dirac $\delta$ function. We use the new dimensionless time variable $t' = (t/t_0)^{1/2}$ and dimensionless invariant $I = I_\phi/S_0$, and rewrite the diffusion equation as

$$\frac{\partial F}{\partial t'} = Dg(t')\frac{\partial}{\partial I}\left(I\frac{\partial F}{\partial I}\right),$$
$$F_{t'=1} = \delta(I-1) \qquad (13)$$

where

$$D = \frac{4\pi\tau S_0\bar{\Gamma}}{\gamma_\phi^2 u\sqrt{k^2\varphi_0/\gamma_0}},$$

$$g(t') = \sqrt{ut_0}t'[1+(ut_0)^2t'^4]^{1/4}\frac{\Gamma(t')}{\bar{\Gamma}}.$$

The function $g(t') \to 1$ as $t' \to \infty$. The constant coefficient $D$ depends only on system parameters ($u, \varphi_0, k, \tau$) and the initial energy of particles $\gamma_0$ [the initial value of the area, $S_0$, depends on $\gamma_0$ and on $\varphi_0$, $k$; see Eq. (6)]. Particles escape from the resonance when $I > t'$ (i.e., $I_\phi > S = S_0\sqrt{t/t_0}$). We solved system (13) numerically and at each time step we excluded from the distribution $F(I,t)$ the part with $I > t'$. We collected these excluded particles as the "exit" distribution $Q$.

The solution of (13) for different moments of time is presented in Fig. 11. One can see that the value of $F(I,t)$ slowly shifts towards large values of $I$ and becomes smoothed (without a central maximum). This is a typical behavior of solutions of diffusionlike equations.

The distribution function of excluded particles $Q$ can be recalculated to the energy distribution for a given moment $t$. Particles escape from the resonance when $I = t' \approx \sqrt{\gamma/\gamma_0}$.

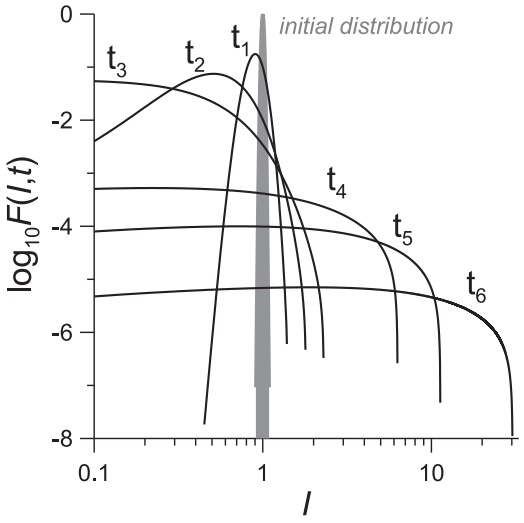


FIG. 11. The distribution function $F(I,t)$ for six moments of time: $t_1 = 1.1t_0$, $t_2 = 1.5t_0$, $t_3 = 2t_0$, $t_4 = 6t_0$, $t_5 = 10t_0$, and $t_6 = 30t_0$. System parameters correspond to magnetic field fluctuations $b_y \neq 0$ with $\sigma_y = 0.08$. The initial distribution is shown by grey color.

For a given moment $t$ we obtain the energy distribution $Q(\gamma)$, which contains all particles escaped from the resonance before this moment. Late in the evolution, when 90% of particles escaped from the resonance, these distributions are shown for three parameter sets in Fig. 12: with $b_y \neq 0$ fluctuations for two values of $\sigma_y$ and with $b_z \neq 0$ fluctuations for one value of $\sigma_z$. Comparison of Fig. 12 with Figs. 6 and 8 shows that distributions $Q(\gamma)$ can reproduce main characteristics of energy distributions obtained by integrating particle trajectories. We observe the maximum of $Q(\gamma)$ distribution for $\sigma_y = 0.08$ at the same energy as was expected from Fig. 8, while the characteristic energies for other distributions are also similar. The distribution of $Q(\gamma)$ has a more gradual tail compared with the profiles shown in Figs. 6 and 8. This is the effect of a finite number of particles in the numerical ensembles used in Figs. 6 and 8: for large $\gamma$ (i.e., large values of energy) when relatively few particles are left in the resonance, the statistics cannot be representative.

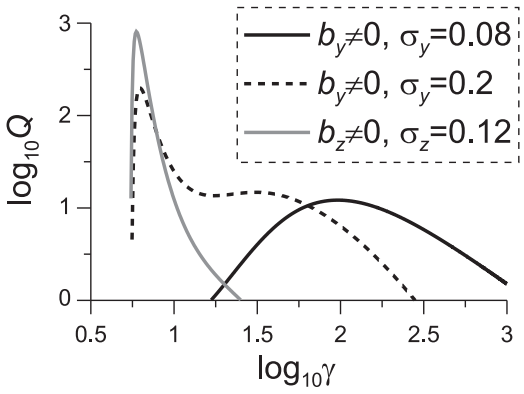


FIG. 12. Energy distributions $Q(\gamma)$ for three systems. $Q(\gamma)$ is renormalized for comparison with Figs. 6 and 8.

## VI. DISCUSSION AND CONCLUSIONS

In the present paper we studied the influence of magnetic field fluctuations on the relativistic surfatron acceleration in a strong electrostatic wave. We restricted our consideration to magnetic field fluctuations along the direction of particle acceleration ($b_y \neq 0$) and along the background magnetic field ($b_z \neq 0$), while fluctuations along the direction of wave propagation ($b_x \neq 0$) are not taken into account. The $B_x$ component of magnetic field cannot be included into the Hamiltonian without introducing the additional degree of freedom, i.e., the corresponding vector potential will have the component $\sim B_x y$ (or $\sim B_x z$). Thus, fluctuations $b_x \neq 0$ can be considered only for the two dimensional system where the canonical momentum $p_y$ (or $p_z$) is not conserved. Although the violation of conservation of $p_y$ occurs only in the presence of random fluctuations (for the unperturbed system we still can use $p_y = \text{const}$), this generalization requires a separate study. Here we only mention that nonzero mean value $\langle b_x \rangle$ of $b_x$ is analogous to the oblique wave propagation when the wave phase is $\phi \sim x\cos\theta + z\sin\theta - ut$ and $\tan\theta \sim \langle b_x \rangle$. The relativistic system with an electrostatic oblique wave was considered in [27]. Surfatron acceleration by oblique electromagnetic waves was considered for nonrelativistic systems [33,34].

Comparison of the obtained dependence of $\mathrm{Var}(\Delta I_\phi)$ on time with the one derived for the nonrelativistic system in [35] shows the main effect of relativistic energies. For the relativistic system we have $\mathrm{Var}(\Delta I_\phi) \sim t^{-1/2}$ (i.e., the more time has passed since the capture, the smaller are typical values of $\Delta I_\phi$ jumps). Therefore, the corresponding diffusive growth of the adiabatic invariant is $\langle I_\phi \rangle \sim t^{1/2}$, which is substantially weaker than the one obtained for the nonrelativistic system $\langle I_\phi \rangle \sim t^{5/2}$ (see [35]). Thus, the process of acceleration of relativistic particles is more stable (robust). This effect can be explained with the help of comparison of Lorentz forces corresponding to magnetic field fluctuations. For the nonrelativistic system the amplitude of this force $\sim v_y \delta B_z \sim ut\delta B_z$ grows with time, while for the relativistic system the corresponding amplitude is finite, $v_y \delta B_z < c\delta B_z$.

Our results were obtained for harmonic waves $\varphi \sim \cos\phi$. However, the same conclusions are valid for nonharmonic waves (e.g., the surfatron mechanism for systems with nonharmonic electrostatic waves was considered in [12,13,41], while nonharmonic electromagnetic waves were considered in [16,24]). It should be noted that the energy distributions obtained in our paper (see Figs. 6 and 8) do not depend on the chosen wave form $\sim\cos\phi$. We considered the acceleration of particles after they were captured by the wave until they escape from the resonance. Thus, we did not take into account the wave periodicity to obtain the energy distributions. As a result, Figs. 6 and 8 represent energy distributions of captured particles even for nonharmonic waves. For nonharmonic (shocklike) waves the ratio $k \gg 1$ means that the thickness of the wave front is smaller than the ion Larmor radius. These conditions are typical for shock waves (see, e.g., review [42] and references therein).

Our results on the stability of surfatron capture relative to fluctuations of the magnetic field point out the robustness of this mechanism of acceleration. The influence of fluctuations on particle acceleration was estimated before for shock waves in [13,43], where fluctuations were produced by a broad spectrum of Alfven waves. We used a simplified model of fluctuations and obtained more general results. We showed that the final energy gained by particles was determined directly by the fluctuation levels $\sigma_{z,y}$. Thus, for small levels of fluctuations of magnetic field ($\sigma_y < 0.1$ and $\sigma_z < \sigma_y^2 < 0.01$) particles can gain substantial energy before escaping from the resonance. These results can be used to describe small groups of high-energy (but still nonrelativistic) ions and relativistic electrons observed in the vicinity of the Earth and Saturn bow shocks [44–46]. In addition, surfatron acceleration by electromagnetic nonlinear waves can be observed close to the region of the magnetic reconnection [16], where shocklike structures are formed by accelerated particle jets [47,48].

In conclusion, we considered the influence of the magnetic field fluctuations on stability of the surfatron capture and acceleration for relativistic charged particles. We showed that fluctuations of the magnetic field component directed along the background magnetic field were the most "dangerous" for surfatron capture, while fluctuations along the wave front did not play so essential a role in particle dynamics [17].

## ACKNOWLEDGMENTS

The work was supported by the RFBR 13-01-00251 (D.V.), by Russian Academy of Science OFN-15 (A.A.), and by the Grants for State Support of Leading Scientific Schools Grant No. NSh-2519.2012.1 (A.N.).

[1] V. D. Shapiro and R. Z. Sagdeev, Phys. Rep. **283**, 49 (1997).
[2] S. Perri, A. Greco, and G. Zimbardo, Geophys. Res. Lett. **36**, 4103 (2009).
[3] D. Shklyar and H. Matsumoto, Surv. Geophys. **30**, 55 (2009).
[4] A. Osmane and A. M. Hamza, Phys. Rev. E **85**, 056410 (2012).
[5] T. Katsouleas and J. M. Dawson, Phys. Rev. Lett. **51**, 392 (1983).
[6] R. Z. Sagdeev and V. D. Shapiro, Sov. J. Exp. Theor. Phys. Lett. **17**, 279 (1973).
[7] R. Z. Sagdeev, *Reviews of Plasma Physics*, 1st ed., Vol. 4 (Consultants Bureau, New York, 1966).
[8] M. A. Malkov and G. M. Zaslavskii, Phys. Lett. A **106**, 257 (1984).
[9] F. Valentini, P. Veltri, and A. Mangeney, Phys. Rev. E **71**, 016402 (2005).
[10] D. Ucer and V. D. Shapiro, Phys. Rev. Lett. **87**, 075001 (2001).
[11] G. P. Zank, H. L. Pauls, I. H. Cairns, and G. M. Webb, J. Geophys. Res. **101**, 457 (1996).
[12] M. A. Lee, V. D. Shapiro, and R. Z. Sagdeev, J. Geophys. Res. **101**, 4777 (1996).
[13] I. Roth and S. D. Bale, J. Geophys. Res. **111**, A07S06 (2006).
[14] G. Zimbardo, Planet. Space Sci. **59**, 468 (2011).
[15] A. V. Artemyev, G. Zimbardo, A. Y. Ukhorskiy, and M. Fujimoto, Astron. Astrophys. **562**, A58 (2014).

[16] A. V. Artemyev, V. N. Lutsenko, and A. A. Petrukovich, Ann. Geophys. **30**, 317 (2012).
[17] N. S. Erokhin, S. S. Moiseev, and R. Z. Sagdeev, Sov. Astron. Lett. **15**, 1 (1989).
[18] T. Amano and M. Hoshino, Astrophys. J. **690**, 244 (2009).
[19] T. Nakamura, K. Mima, H. Sakagami, and T. Johzaki, Phys. Plasmas **14**, 053112 (2007).
[20] S. Takeuchi, K. Sakai, M. Matsumoto, and R. Sugihara, Phys. Lett. A **122**, 257 (1987).
[21] A. A. Chernikov, G. Schmidt, and A. I. Neishtadt, Phys. Rev. Lett. **68**, 1507 (1992).
[22] A. I. Neishtadt, A. V. Artemyev, L. M. Zelenyi, and D. L. Vainshtein, JETP Lett. **89**, 441 (2009).
[23] N. Yugami, K. Kikuta, and Y. Nishida, Phys. Rev. Lett. **76**, 1635 (1996).
[24] S. Takeuchi, Phys. Plasmas **12**, 102901 (2005).
[25] A. V. Artemyev, A. I. Neishtadt, L. M. Zelenyi, and D. L. Vainchtein, Chaos **20**, 043128 (2010).
[26] A. I. Neishtadt, B. A. Petrovichev, and A. A. Chernikov, Sov. J. Plasma Phys. **15**, 1021 (1989).
[27] A. P. Itin, A. I. Neishtadt, and A. A. Vasiliev, Physica D: Nonlin. Phenom. **141**, 281 (2000).
[28] A. N. Erokhin, N. S. Erokhin, and V. P. Milant'ev, Plasma Phys. Rep. **38**, 396 (2012).
[29] S. V. Bulanov and A. S. Sakharov, Sov. J. Exp. Theor. Phys. Lett. **44**, 543 (1986).
[30] D. L. Vainchtein, E. V. Rovinsky, L. M. Zelenyi, and A. I. Neishtadt, J. Nonlinear Sci. **14**, 173 (2004).
[31] Y. Kuramitsu and V. Krasnoselskikh, Phys. Rev. Lett. **94**, 031102 (2005).
[32] A. P. Itin, Plasma Phys. Rep. **28**, 592 (2002).
[33] A. Vasiliev, A. Neishtadt, and A. Artemyev, Phys. Lett. A **375**, 3075 (2011).
[34] S. Takeuchi, Phys. Plasmas **19**, 070703 (2012).
[35] A. Artemyev, D. Vainchtein, A. Neishtadt, and L. Zelenyi, Phys. Rev. E **84**, 046213 (2011).
[36] G. Zimbardo, A. Greco, L. Sorriso-Valvo, S. Perri, Z. Vörös, G. Aburjania, K. Chargazia, and O. Alexandrova, Space Sci. Rev. **156**, 89 (2010).
[37] A. J. Hull, L. Muschietti, M. Oka, D. E. Larson, F. S. Mozer, C. C. Chaston, J. W. Bonnell, and G. B. Hospodarsky, J. Geophys. Res. **117**, A12104 (2012).
[38] L. B. Wilson, A. Koval, A. Szabo, A. Breneman, C. A. Cattell, K. Goetz, P. J. Kellogg, K. Kersten, J. C. Kasper, B. A. Maruca, and M. Pulupa, J. Geophys. Res. **118**, 5 (2013).
[39] P. H. Diamond, S.-I. Itoh, and K. Itoh, *Modern Plasma Physics* (Cambridge University Press, Cambridge, England, 2010).
[40] L. D. Landau and E. M. Lifshitz, *Vol. 1: Mechanics*, Course of Theoretical Physics (Pergamon, Oxford, 1988).
[41] A. A. Vasiliev, in *Advance in Plasma Physics*, Vol. 5 (Nova Science Publishers, Hauppauge, NY, 2002), pp. 129–132.
[42] V. Krasnoselskikh, M. Balikhin, S. N. Walker, S. Schwartz, D. Sundkvist, V. Lobzin, M. Gedalin, S. D. Bale, F. Mozer, J. Soucek, Y. Hobara, and H. Comisel, Space Sci. Rev. **178**, 535 (2013).
[43] R. B. Decker and L. Vlahos, J. Geophys. Res. **90**, 47 (1985).
[44] V. N. Lutsenko and K. Kudela, Geophys. Res. Lett. **26**, 413 (1999).
[45] A. Klassen, R. Gómez-Herrero, R. Müller-Mellin, S. Böttcher, B. Heber, R. Wimmer-Schweingruber, and G. M. Mason, Ann. Geophys. **27**, 2077 (2009).
[46] A. Masters, L. Stawarz, M. Fujimoto, S. J. Schwartz, N. Sergis, M. F. Thomsen, A. Retinò, H. Hasegawa, B. Zieger, G. R. Lewis, A. J. Coates, P. Canu, and M. K. Dougherty, Nat. Phys. **9**, 164 (2013).
[47] M. Hoshino, T. Mukai, I. Shinohara, Y. Saito, and S. Kokubun, J. Geophys. Res. **105**, 337 (2000).
[48] M. I. Sitnov, M. Swisdak, and A. V. Divin, J. Geophys. Res. **114**, A04202 (2009).